Effects of interfacial atomic segregation and intermixing on the electronic properties of InAs/GaSb superlattices

Rita Magri
Istituto Nazionale per la Fisica della Materia e Dipartimento di Fisica, Universitá

tween the first light-hole $lh1$ state and the second heavy-hole state $hh2$ and, respectively, between the first heavy-hole state and the first electron state $e1$ are already nonzero by symmetry, $V_{lh1\text{-}hh2}(\mathbf{k}_\parallel=0)\neq 0$ and $V_{hh1\text{-}e1}(\mathbf{k}_\parallel=0)\neq 0$ at zero in-plane momentum ($\mathbf{k}_\parallel=0$). Consequently, (a) if $lh1$ and $hh2$ approach degeneracy, the $lh1$ and $hh2$ levels anticross (as opposed to cross) at some critical superlattice period [$\approx$60 ML for $(AlAs)_n/(GaAs)_n$ (Ref. 4) and $\approx$15 ML for $(InAs)_n/(GaSb)_n$ (Ref. 1)]; (b) the transitions $lh1\leftrightarrow e2$ and $hh2\leftrightarrow e1$ become dipole allowed; (c) $hh1$ will anticross $e1$. In InAs/GaSb this occurs at $\approx$28 ML (Ref. 5) (see also inset to Fig. 1). (a), (b), and (c) do not occur if the coupling potentials $V_{lh1\text{-}hh2}(\mathbf{k}_\parallel=0)$ and $V_{hh1\text{-}e1}(\mathbf{k}_\parallel=0)$ are zero, as is the case in the conventional eight-band $\mathbf{k}\cdot\mathbf{p}$ model[6] which does not "see" the correct atomistic C_{2v} or D_{2d} symmetry, confusing it with T_d. Thus, conventional eight-band $\mathbf{k}\cdot\mathbf{p}$ models give *crossing* of $lh1$ and $hh2$, or $hh1$ and $e1$, and dipole *forbidden* $lh1\leftrightarrow e2$ and $hh2\leftrightarrow e1$ transitions.

(ii) *Coupling of lh1 and hh1 at* $\mathbf{k}_\parallel=0$. In common-atom superlattices with equivalent interfaces, this coupling vanishes at $\mathbf{k}_\parallel=0$. However, in no-common-atom superlattices with inequivalent interfaces $V_{lh1\text{-}hh1}(\mathbf{k}_\parallel=0)\neq 0$ by symmetry. Consequently, (a) if $lh1$ and $hh1$ approach degeneracy $lh1$ will anticross (as opposed to cross) $hh1$. (b) The $e1\leftrightarrow hh1$ and $e1\leftrightarrow lh1$ transitions develop an in-plane polarization anisotropy whereby the dipole transitions have unequal strength along the [110] and [$-$110] in-plane directions.[1,7,8] Effects (a) and (b) are unique to C_{2v} superlattices with inequivalent interfaces and are expected to drastically change as the superlattice interfaces are modified.

(iii) *Interfacial "spikes" in the band allignments*. Since both the "normal" interface and the "inverted interface" manifest fundamentally new types of chemical bonds (Ga-As and In-Sb, respectively) absent in the constituent binary compounds (InAs and GaSb), we expect such bonds to have their own band offsets. Pseudopotential calculations[9] indeed show considerable local variations ("spikes") in the band offsets across these interfaces. In particular, the In-Sb strained layer has a rather high hh VBM [230 meV above GaSb (Ref. 1)] which can act as a hole trap. These interfacial potential spikes must naturally be sensitive to the interfacial composition and intermixing.

The foregoing discussion highlights the importance of studying interfacial morphology in no-common-atom superlattices, where the interfacial symmetry of abrupt structures mandates unique electronic properties. There are a number of experimental reasons to consider the interfacial morphology of such superlattices and their effects on the electronic properties. First, the known tendency[3] of Sb to surface segregate relative to As and the tendency of In to segregate relative to Ga suggests possible disorder effects on interfacial morphology. Second, recent cross-sectional scanning tunneling microscopy (STM) measurements on InAs/GaSb superlattices observed directly Sb penetration into the first few InAs monolayers.[3] Third, there are conspicuous changes in the band gaps of InAs/GaSb superlattices that are observed in samples grown at slightly different conditions. These unexpectedly large effects could arise from different interfacial morphology. For example, Yang *et al.*[10] found a 30 meV

a gap $E_g = 253$ meV was measured for a sample with only Ga-As interfacial bonds, with a difference of about 40 meV.[12]

(i) Dente and Tilton used a *discrete* screened potential $v_\alpha(\mathbf{G}_i)$ available only at few reciprocal lattice vectors $\mathbf{G}_i$ of the two binary compounds GaSb and InAs. Instead, we fit directly a *continous* $v_\alpha(\mathbf{q})$ to all four binary compounds (GaSb, InAs, GaAs, InSb), whose bonds are present in the superlattice (Appendix) and do not make any special assumption about the shape of the interface potential: the interfacial Ga-As and In-Sb bonds are treated individually, each bond having its own band offset with respect to its environment.

(ii) We use an explicitly strain-dependent pseudopotential $v_\alpha(\mathbf{q},\epsilon)$, whereas Dente and Tilton used a strain-independent potential $v_\alpha(\mathbf{G}_i)$ and applied slight form factor adjustments to the InAs potential to fit the band gap of the strained material. However, the strain-dependent $v_\alpha(\mathbf{q},\epsilon)$ was previously shown[22] to be crucial for correctly describing strained bonds. In fact, the Ga-As and In-Sb bonds at the interfaces of the InAs/GaSb SL differ by 14%, while the lattice mismatch of either GaAs and InSb with respect to InAs and GaSb is 6%–7%.

(iii) Dente and Tilton do not model the pseudopotential of the alloys that could exist in this system, e.g., GaAsSb, GaInAs, GaInSb, and InAsSb, whereas in our method they are explicitly described (Appendix).

The differences in the methods produces by necessity different results for the superlattices, even though the bulk compounds are described similarly. For example in the $(InAs)_8/(GaSb)_m$ superlattices we (Dente and Tilton) get gaps of 238 meV (290 meV), 281 meV (314 meV), 305 meV (326 meV), and 325 meV (338 meV) for $m=8$, 12, 16, and 24, respectively.

Another strain-dependent empirical pseudopotential method for InAs/GaSb has been recently proposed by Shaw *et al.*[23,24] The inclusion of the strain dependence in the pseudopotential form factors is conceptually similar to that used in our scheme[16] [compare Eq. (5) of Ref. 20 with Eqs. (A1) and (A3) in the Appendix], but the method is implemented differently. In our case the use of a continous momentum $\mathbf{q}$ function $v_\alpha(\mathbf{q},\epsilon)$ reduces the number of parameters that have to be fit and produces authomatically the strained form factors at all the appropriate superlattice wave vectors $\mathbf{G}_i$. Shaw *et al.*[23,24] construct, instead, the strained potential $V(\mathbf{G}_i)$ through a direct numerical interpolation between the form factors corresponding to a series of hydrostatic strains. A more significant difference between our method and that of Ref. 24, is in the description of the interfacial bonds. In our method we use specific atomic pseudopotentials to describe the Ga-As and In-Sb interfacial bonds with respect to the In-As and Ga-Sb bulk compounds (see the Appendix) We have found it essential for obtaining a good description of the alloy positive band bowings. No special treatment of the different interfacial bonds is presented in Refs. 23 and 24.

III. ABRUPT $(InAs)_n/(GaSb)_m$ (001) SUPERLATTICES

A. Symmetric $(InAs)_n/(GaSb)_n$

Figure 1(a) shows the electron $e1$ and hole ($hh1$, $lh1$, $hh2$) levels of symmetric $(InAs)_n/(GaSb)_n$ (001) superlattices as a function of n. We see that as n is reduced from infinity, the $e1$ level moves up, while $hh1$, $lh1$, and $hh2$ move down, all states becoming more and more confined within the corresponding wells. When $n<28$ the superlattices acquire a semiconducting gap with the first electron state $e1$ localized in the InAs layer and the first hole state $hh1$ localized in the GaSb layer. At $n=28$ the energy of the $e1$ level becomes lower than the energy of the hole $hh1$ state. However, the expected metallization of the system does not occur because of the opening of the anticrossing gap. The calculated anticrossing gap at $k_\parallel=0$ is $E_A^{hh1,e1}=11$ meV (inset to Fig. 1). We find a strong wave function mixing at the $hh1$-$e1$ anticrossing, in good agreement with experiment[25] and other calculations.[21]

In addition to $e1$-$hh1$ coupling and anticrossing we find also anticrossing between the hole levels $lh1$ and $hh2$ around $n=13$. For superlattice periods n close to $n=13$ the wave functions of the two hole states strongly intermix. The calculated anticrossing gap is $E_A^{lh1,hh2}=40$ meV. This causes the appearance of new transitions $lh1\leftrightarrow e2$ and $hh2\leftrightarrow e1$ in the spectra that become allowed because of this mixing.

B. Asymmetric $(InAs)_8/(GaSb)_m$

Figure 1(b) shows the electron and hole states of $(InAs)_8/(GaSb)_n$ (001) SL's vs n. While the hole states move to higher energies as the thickness n of the GaSb barrier increases, [as is the case in Fig. 1(a) for symmetric $(InAs)_n/(GaSb)_n$], we see in Fig. 1(b) that also the electron state moves to *higher* energies as n increases, opposite to Fig. 1(a). The net effect is a blueshift of the band gap.

The reason for the blueshift[26] is as follows: the energy of the $hh1$ hole state moves upward as n increases and its wave function becomes less and less confined. This effect goes in the direction of *diminishing* the fundamental gap. However, the gap *increases*, instead, because the energy of the first electron state $e1$ moves upwards as n increases, by a larger amount. This is so because the wave function of the electron state becomes more and more confined in the InAs well as the thicker GaSb layer provides a larger barrier for the electron states and diminishes the interaction between electron states in subsequent InAs wells. It is indeed the coupling between the $e1$ states of neighboring InAs wells that pushes down the energy of the $e1$ ''bonding'' electron states in superlattices with short GaSb barriers.

The calculated transition energies at Γ from the various valence subbands to the lowest conduction subband are reported in Table I, where they are compared with the values deduces from the absorbance spectroscopy results of Kaspi *et al.*[26] The comparison is only tentative, because the procedure of extracting sharp transition energies from broad absorption spectra has some uncertainties. Nevertheless, the interband transitions seen by the experiment are predicted reasonably well by our calculations, in particular the blueshift observed for the energy of the first transition when the GaSb thickness is increased. The measured samples we are comparing our calculations with in Table I have been grown with particular attention to minimize imperfections like in-

teratomic diffusion and segregation during the growth and interfacial broadening, obtaining high-quality superlattices very close to the abrupt model, as successive characterizations have shown.[26] However, it is impossible to eliminate completely these imperfections and grow perfectly abrupt interfaces. It is then important to assess how the imperfections can modify the results we have obtained for the perfect geometry and recompare with experiment.

IV. SINGLE-LAYER MODEL OF INTERFACIAL DISORDER

A. Model

Our first model of interfacial disorder aims at transforming simply and continuously the C_{2v} system with two unequal interfaces [Eqs. (1) and (2)] to a D_{2d} system with equal interfaces. We do this as follows. We observe first that if in the plane sequence of Eq. (1) of the InAs-on-GaSb interface we change the interface As plane into a Sb plane, then we trasform the Ga-As interface into a In-Sb interface. If we leave the other interface sequence, that of Eq. (2), unchanged, we end up with a superlattice having a noninteger number of layers $(InAs)_{7.5}/(GaSb)_{8.5}$, with two *equivalent* In-Sb interfaces. We denote this configuration as $(InAs)_7$-In-Sb-$(GaSb)_8$ to stress the presence of an extra In-Sb interface. In a similar way, we can change the Sb plane at the GaSb-on-InAs interface [sequence of Eq. (2)] into an As plane, leaving the other interface, the sequence of Eq. (1), unchanged. The resulting SL has now two *equivalent* Ga-As interfaces. We indicate this $(InAs)_{8.5}/(GaSb)_{7.5}$ SL configuration as $(GaSb)_7$-Ga-As-$(InAs)_8$.

By denoting the fraction of Sb atoms at the interfacial anion plane i ($i=1$ for the normal interface, $i=2$ for the inverted interface), as $x_I^{(i)}$, we have the following.

(1) $(InAs)_8/(GaSb)_8$ [$x_I^{(1)}=0$ (Ga-As bonds) at the InAs-on-GaSb interface and $x_I^{(2)}=1$ (In-Sb bonds) at the GaSb-on-InAs interface].

(2) $(InAs)_7$-In-Sb-$(GaSb)_8$ [to $x_I^{(1)}=1$ (In-Sb bonds) at the InAs-on-GaSb interface and $x_I^{(2)}=1$ (In-Sb bonds) at the GaSb-on-InAs interface].

(3) $(GaSb)_7$-Ga-As-$(InAs)_8$ [$x_I^{(1)}=0$ (Ga-As bonds) at the InAs-on-GaSb interface and $x_I^{(2)}=0$ (Ga-As bonds) at the GaSb-on-InAs interface].

By inserting mixed $Sb_{x_I}As_{1-x_I}$ layers we can vary gradually the interfacial composition and change continuously $x_I^{(i)}$ ($0<x_I^{(i)}<1$). To generate configurations with fractional interfacial composition we use a larger surface unit cell. The interface unit cell is shown in Fig. 2. It is a 4×4 interface unit cell in the substrate plane, containing 16 primitive unit cells. In figure we show also the projection onto the (001) interface of the standard cubic unit cell. We obtain different interfacial configurations x_I by occupying differently the 16 planar sites with Sb and As atoms. Thus, all the configura-

B. Results for the single-layer model of interfacial disorder:

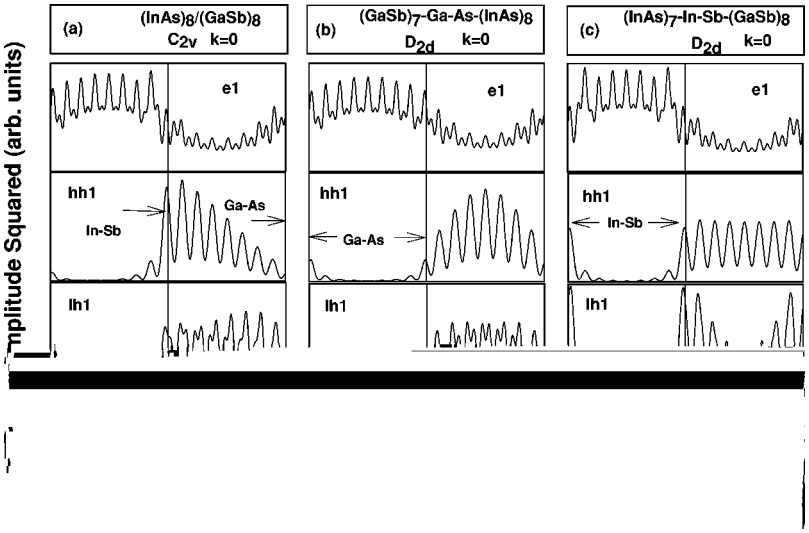

FIG. 4. In-plane averaged wave function amplitude squared of the $e1$, $hh1$, $lh1$, and $hh2$ states at the Brillouin zone center for the (a) $(InAs)_8/(GaSb)_8$, (b) $(GaSb)_7$-Ga-As-$(InAs)_8$, and (c) $(InAs)_7$-In-Sb-$(GaSb)_8$ superlattices. The arrows indicate the composition of the related interfacial bonds.

Figure 5 shows the calculated dipole transition elements of the $hh1 \rightarrow e1$ transition at $k=(0.02,0.02,0)2\pi/a$ and at $k=(-0.02,0.02,0)2\pi/a$ for the three superlattices. We can see the following: (i) the transition strengths strongly depend on the polarization of the radiation (001) vs (110) or (−110); (ii) there is a strong anisotropy between the transitions with polarization along the two in-plane directions [110] and [−110], respectively, for all the superlattices and for both k vectors; and (iii) the in-plane polarization anisotropy of the D_{2d} symmetry superlattices at $k=\alpha[110]$ is *exactly* compensated by the anisotropy at $k=\alpha[-110]$, so that the integration over the entire BZ gives a net zero anisotropy consistent with the D_{2d} symmetry. This compensation does not occur in the case of the superlattice with C_{2v} symmetry, where a residual in-plane polarization anisotropy is expected after integration over the entire BZ.

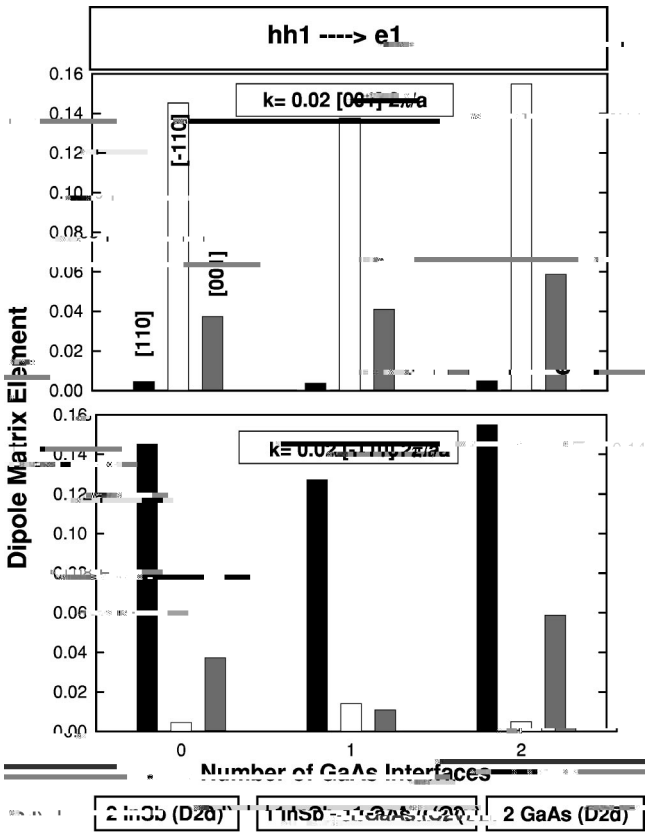

FIG. 5. Dipole matrix elements of the $hh1 \leftrightarrow e1$ interband transition for $(InAs)_7$-In-Sb-$(GaSb)_8$ (zero Ga-As interfaces), $(InAs)_8/(GaSb)_8$ (one Ga-As interface), and $(GaSb)_7$-Ga-As-$(InAs)_8$ (two Ga-As interfaces), calculated at two k points of the Brillouin zone, one along the [110] direction, the other along the [−110] direction. The dipole matrix elements are relative to different directions of the radiation polarization: [110], [−110], and [001].

C. Results for the single-layer model: Intermixed $Sb_{x_I}As_{1-x_I}$ interfaces

Figure 6 reports the energies of the $hh1 \rightarrow e1$, $lh1 \rightarrow e1$, and $hh2 \rightarrow e1$ interband transitions at the BZ center as a function of the number of interfacial Ga-As bonds or as a function of the total As content, $1-x$. For each value of As interfacial composition $1-x_I$ we average over a few in-plane configurations corresponding to different occupations of the interface plane sites (see Fig. 2). The dependence of the interband transition energies on the particular in-plane atomic configuration for the same composition x_I is small, about an order of magnitude smaller than the difference between the transition energies of superlattices with different interface composition. We see in Fig. 6 that (i) the energies of all transitions increase with the number of interfacial Ga-As bonds. (ii) While for the $lh1 \rightarrow e1$ transition the trend is approximately linear and with small slope, in the case of the transitions involving the heavy-hole states, deviations from linearity are observed and the slopes are larger: for the $hh2 \rightarrow e1$ transition the total increase of the transition energy with the Ga-As interfacial bonds is quite large, 146 meV, and for the $hh1 \rightarrow e1$ transition is only 50 meV. The smaller sensitivity of the $hh1 \rightarrow e1$ transition energy is due to the strong localization of the $hh1$ wave function at the In-Sb bonds which pins the energy of the $hh1$ level. Indeed, since the position of the electron state $e1$ moves up linearly with the

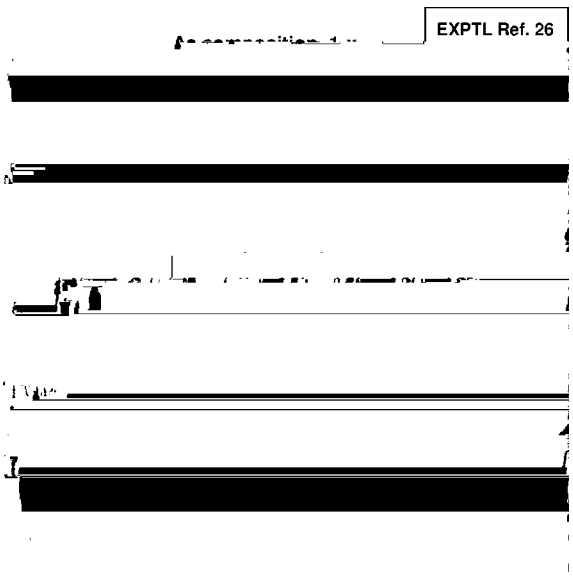

FIG. 6. Calculated energies of the first three interband transitions at the Brillouin zone center versus the number of Ga-As interfaces and the total As fraction in the superlattices. At the right end side the experimental data from Ref. 26 are given for comparison. We disagree with the assignment $hh2 \leftrightarrow e1$ of the third transition.

increase of Ga-As interfacial bonds, the behavior shown in Fig. 6 for the transition energies reflects mainly the shifts of the heavy-hole levels. (iii) While the agreement with the experiment[26] for the first two transitions is good, we disagree with the assignment of the third transition at 670 meV to $hh2 \leftrightarrow e1$. We will come back to this point again in Sec. V.

Figure 7 gives the dipole matrix elements of the $hh1 \rightarrow e1$, $lh1 \rightarrow e1$, and $hh2 \rightarrow e1$ transitions at the BZ center for polarization directions along the superlattice growth [001] axis and the two in-plane [110] and [−110] axes as a function of the number of Ga-As interfacial bonds. We can see that (1) in the case of the $hh1 \rightarrow e1$ transition, the total oscillator strength is higher for the two D_{2d} structures with zero Ga-As interfacial bonds and with two Ga-As interfaces, than for the C_{2v} structure with only one Ga-As interface.

(2) The in-plane polarization anisotropy is higher in the case of the C_{2v} superlattice. We can conclude, therefore, that a larger inequality of the interfacial bonds at the two subsequent interfaces leads to a larger in-plane polarization anisotropy.

(3) In the case of the $lh1 \rightarrow e1$ transition there is a switch in magnitude of the oscillator strengths of the [110] and [−110] polarizations and the oscillator strength is much larger for the [001] polarization than for in-plane polarization. The total (and [001]-polarized) transition probability increases with the number of Ga-As interfacial bonds.

(4) The intensity of the $lh1 \rightarrow e1$ total oscillator strength [Fig. 7(b)] is anticorrelated to that of the $hh2 \rightarrow e1$ transition [Fig. 7(c)]. The $hh2 \rightarrow e1$ transition is parity forbidden in the standard envelope function theory but it can gain some finite probability through the mixing of $hh2$ with $lh1$. [For this reason we do not believe that the observed[26] transition at 670 meV was correctly assigned to the $hh2 \rightarrow e1$ transition (see Fig. 6).] The total dipole strength of the $hh2 \rightarrow e1$ transition diminishes with the increase of Ga-As interfacial bonds. The intensity of the $hh2 \rightarrow e1$ is exactly opposite with respect to the dipole strength of the $lh1 \rightarrow e1$ transition. This means that the $lh1$-$hh2$ coupling is larger in the case of the two In-Sb interfaces than in the case of the two Ga-As interfaces. Also, for structures having an excess of In-Sb bonds at both interfaces (Sb-rich structures), the in-plane polarized $hh2 \leftrightarrow e1$ transition acquires some magnitude and a strong anisotropy between the [110] and [−110] directions (except

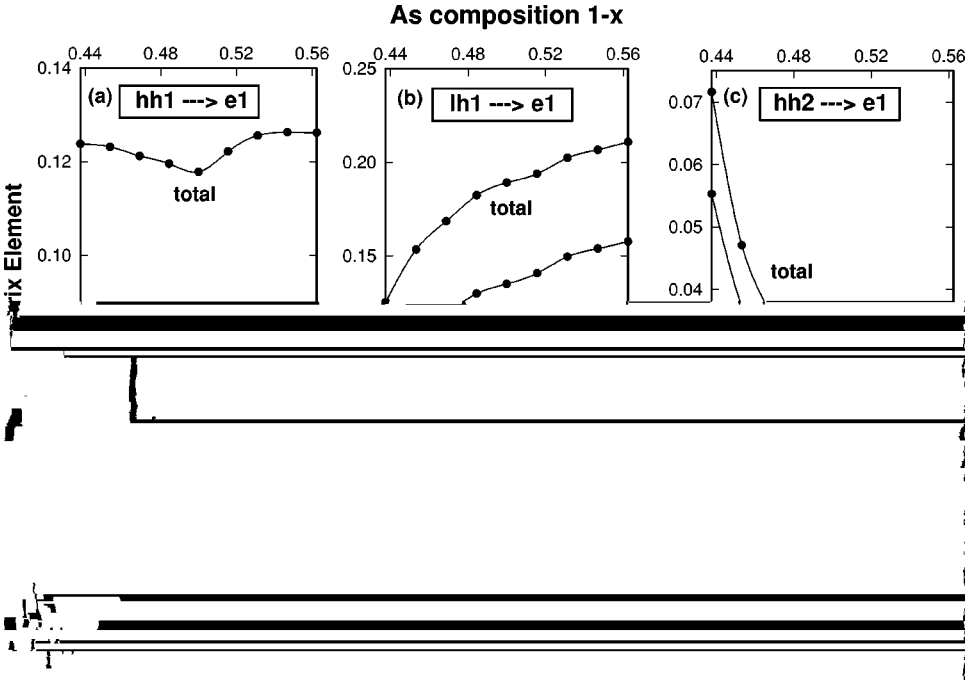

FIG. 7. Total and polarization resolved (along the [110], [−110], and [001] directions) dipole matrix elements of the $hh1 \leftrightarrow e1$, $lh1 \leftrightarrow e1$, and $hh2 \leftrightarrow e1$ interband transitions vs the number of Ga-As interfaces and the total As fraction in the superlattices.

the D_{2d} structure which has zero polarization anisotropy). This observation shows that there is a definite dependence of the $lh1$-$hh2$ band coupling on the nature of the interface bonds.

A comparison of the polarization ratios

$$\rho_{i,j}=\frac{P^{i,j}_{110}-P^{i,j}_{-110}}{P^{i,j}_{110}+P^{i,j}_{-110}} \quad (4)$$

where P indicates the transition dipole oscillator strength of transition $i\rightarrow j$) of the $hh1\rightarrow e1$ and $lh1\rightarrow e1$ transitions can also shed some light on the composition of the interfacial bonds. In Table II we give the calculated polarization ratios $|\rho|$ of the $hh1\leftrightarrow e1$ and $lh1\leftrightarrow e1$ transitions for one structure for each $\{x_I^{(i)}\}$ value. We observe that the following.

(i) The polarization ratios of the $lh1\leftrightarrow e1$ transitions are always larger than those of the $hh1\leftrightarrow e1$ transitions.

(ii) A very small ($\rho<0.05$) polarization ratio of $hh1\leftrightarrow e1$ means that the two interfaces of the superlattice have approximately the same bonds.

(iii) A ratio between the magnitude of the polarization ratios of the $hh1\leftrightarrow e1$ and of the $lh1\leftrightarrow e1$ transitions, given in Table II, larger than 0.4 is an indication that the structure is Sb rich with a larger number of interfacial In-Sb bonds than of Ga-As bonds.

In this section we have seen that the nature of the interfacial bonds in the no-common-atom superlattices has a strong effect on the in-plane polarization anisotropy of the single interband transitions. We will see next that also segregation affects the energies and the in-plane polarization anisotropy of the transitions.

V. KINETIC GROWTH MODEL OF SEGREGATION

A. Model

While the single-layer model of interfacial disorder clarifies the role of the interfacial bond symmetries on the electronic structure and the interband transitions, it does not take into account the effects of atomic segregation, diffusion, and cross incorporation occurring during sample growth. To generate composition profiles for GaSb/InAs superlattices we have relied on a kinetic model for MBE growth, first introduced by Dehaese *et al.*[27] which we have extended to treat simultaneously the segregation of both group-III and

term is the rate of A atoms leaving the surface after exchanging with bulk B atoms. The conservation of A atoms and of the total number of surface atoms at any time t leads to the conditions

$$x_A^s(t)+x_A^b(t)=x_A^s(0)+x_A^b(0)+\Phi_A t, \qquad (7)$$

$$x_A^s(t)+x_B^s(t)=x_A^s(0)+x_B^s(0)+(\Phi_A+\Phi_B)t, \qquad (8)$$

and, at any t, we have $x_A^b(t)+x_B^b(t)=1$. A small fraction x_0 of the segregating Sb specie is incorporated into each InAs layer during the growth because of an unwanted vapor background. This cross incorporation has been taken into account modifying slightly the fluxes Φ_{As} and Φ_{Sb} during the growth of InAs so as to have the incorporation of a small constant Sb fraction $x_0=0.015$ into each InAs layer, as proposed in Ref. 3. Our approximations are the following: (i) the barrier energies, Eq. (5), for atomic exchanges are assumed to be independent of the atomic species surrounding the exchanging atoms, (ii) surface reconstructions during growth are neglected, and (iii) surface roughness and the lateral disorder related to steps are also neglected.

We solve numerically Eqs. (6)–(8) for $A=$ Ga, In, As, and

tice matched to a GaSb substrate. While we have modeled the profile along the [001] growth direction no experimental information is available on the atomistic arrangement in the perpendicular substrate (001)

Figure 10 shows the interband transition energies as a function of the superlattice growth temperature for the $(InAs)_8/(GaSb)_8$ superlattice. At the far left we have reported the calculated energies of the abrupt superlattice by squares, while the experimental absorbance data of Kaspi *et al.*[26] are shown with thick horizontal bars. For each growth temperature ,and, thus, for the same segregation profile along the growth direction) we have calculated three structures which differ only for the in-plane atomic arrangement. We see that the following.

,1) A segregation-induced steep *increase* ,blueshift) of the

and,.j /F15l[(p62371.15 TD(Tshifn0001 Tc (26)Tj 9.978 0 0 8.7(477 585.5

Δ Σ ϵ ϵ ϵ Φ Φ ψΣ ϵ ϵ

$\Delta_{In/Ga}$ for cation segregation and a small $\Delta_{Sb/As}$ for anion segregation causes the narrowing of the InAs electron well with increasing T_g.

C. Results for the electronic and optical properties of segregated superlattices

In this subsection we analyze the consequences on the electronic and optical properties of the segregation-induced modification of the superlattice profile along the growth direction.

In Ref. 29 we studied the implications of segregation on the wave functions. In that paper we compared the amplitudes of the $hh1$ hole wave functions of the $(InAs)_8/(GaSb)_{16}$ superlattice for the abrupt geometry and for the structure grown at $T_g = 525\,^{\circ}C$. The amplitude of the $hh1$ wave function, which is much larger on the In-Sb ,inverted) interface than on the Ga-As ,normal) interface in the abrupt geometry [see Fig. 4,a)], is substantially reduced by segregation. The wave function amplitude becomes similar at the two interfaces. Segregation affects to a lesser degree also the $lh1$ and $e1$ wave functions, which remain closer to the abrupt case ,see Fig. 4).

ML. Because of the anion smaller segregation energy, the penetration length of Sb into InAs is much smaller.

3) The inverted interface is less broadened but In and, at a larger growth temperature, As segregation leads to a 1 ML shift of the interface backward into the InAs well. As a consequence the InAs electron well becomes 1 ML narrower.

Finally, we have studied the consequences of the changes in the superlattice profiles and of the interfacial disorder on the electronic properties, applying the empirical pseudopotential method. We have found.3

scription of the Ga-As and In-Sb interface bonds we have

and gaps of the four binary compounds are in excellent

The atomic positions are relaxed using the valence force field expression

$$E = \sum_i \frac{3}{8\, d_{0i}^2} \alpha_{i'} \mathbf{r}_i \cdot \mathbf{r}_i - d_{0i}^2)^2$$

nevetheless good. The deviations are within 0.1 for $In_{0.5}Ga_{0.5}As$, $In_{0.5}Ga_{0.5}Sb$, and $InAs_{0.5}Sb_{0.5}$. Only for the $GaAs_{0.5}Sb_{0.5}$ alloy is the calculated bowing, 0.53 eV, definetely smaller than the experimental value $>$1.0 eV.

[29] R. Magri and A. Zunger, Phys. Rev. B **64**, R081305 (2001).
[30] J. Harper, M. Weimer, D. Zhang, C.-H. Lin, and S.S. Pei, Appl. Phys. Lett. **73**, 2805 (1998).
[31] M. Weimer (private communication).
[32] R.M. Feenstra, D.A. Collins, D.Z.Y. Ting, M.W. Wang, and T.C. McGill, Phys. Rev. Lett. **72**, 2749 (1994).
[33] M.E. Twigg, B.R. Bennett, P.M. Thibado, B.V. Shanabrook, and L.J. Whitman, Philos. Mag. A **7**, 7 (1998).